

High-density sphere packing for discrete element method simulations

Carlos Labra^{*,†} and Eugenio Oñate

*International Center for Numerical Methods in Engineering, Technical University of Catalonia,
Gran Capitan s/n, 08034 Barcelona, Spain*

SUMMARY

The first step in a discrete element simulation is the discretization of the domain into a set of particles. The cost of generating a good cylindrical or spherical packing has resulted in a great number of approaches during the last years. A new algorithm is proposed for high-density packing using a scheme that minimizes the distance between each particle. Using the support of a finite element mesh, less time is needed in order to achieve a low porosity configuration. In addition, a boundary constraint is introduced. The application of the same optimization scheme is used as a condition to force a good surface definition. The results obtained show a high efficiency for the generation of low porosity packing, achieving values smaller than 10% in 2D cases and 30% in 3D cases. Copyright © 2008 John Wiley & Sons, Ltd.

Received 18 April 2008; Revised 29 July 2008; Accepted 15 September 2008

KEY WORDS: sphere packing; discrete elements; mesh generation

1. INTRODUCTION

In the last years, the discrete element method (DEM) has become an useful tool for the simulation of geomechanics and particle movement processes [1–4]. The technique requires the discretization of the media by a finite set of particles. For some applications, such as wear analysis of mechanical parts or impact analysis, a good compaction rate is crucial [5–7]. In these cases the generation of a sufficiently dense distribution of particles presents a major challenge. A number of approaches have been developed for the generation of cylindrical (2D) and spherical (3D) particles.

The so-called *geometrical algorithms* face the problem of using purely geometrical considerations. An example is the algorithm used in the PFC2D code [8], where the particle position and

*Correspondence to: Carlos Labra, International Center for Numerical Methods in Engineering, Technical University of Catalonia, Gran Capitan s/n, 08034 Barcelona, Spain.

†E-mail: clabra@cimne.upc.edu

Contract/grant sponsor: Publishing Arts Research Council; contract/grant number: 98-1846389

size are obtained by a random number. If overlapping occurs, a new random location is achieved with the same fixed radius. Similar schemes are proposed by Lin and Ng [9] and Evans [10]. In [8] it is proposed an alternative modification of the algorithm, where the radii of all particles are expanded by the same factor. The generation stops when contacts are found. These schemes are called *lily-pond models* [11]. The *Stienen Model* [12] uses a random location to calculate the radius of the particles by half of the mean distance to neighbouring particles. The algorithm used by Cui and O'Sullivan [13] is an example of this technique where the circumcenter (2D), or circumsphere (3D) and the vertex are used for locating the particles, and their radii are calculated by the distance between the neighbouring particles. More examples of this and other techniques can be found in [12].

Recently, more sophisticated generation algorithms were proposed, like the *advancing front method* proposed by Feng *et al.* [14] and Lohner and Oñate [15], where the particle locations are calculated on the basis of previous particle inclusions within a predetermined radius. All of these methods guarantee a very high generation velocity, although the density is however usually low.

Another category of techniques is based on the so-called *dynamic algorithms*, where external helps are used, like body forces or DEM simulations, in order to find better values of densities. Normally, the same DEM code is used in order to obtain a good final packing of rigid particles with the predefined radius. The radii are selected using some distribution and the media is filled using gravity forces. Some examples of this can be found in [16]. Other schemes, like the one proposed by Han *et al.* [17], use an iterative compression algorithm for the density modifications. The use of this set of techniques requires an initial generation, and some of the *geometrical algorithms* are typically used. These techniques can result in dense distributions, with significantly high computational costs.

The present work proposes an alternative technique for the generation of very dense particle distributions. The idea is to use a fast algorithm for an initial generation, like some of the ones presented previously and densify the package by an optimization algorithm. In particular, a finite element mesh (FEM)-based scheme is used, similar to the *Stienen Model* [12].

2. THE ALGORITHM

The main idea of this method is to *improve* a given particle assembly in order to obtain a lower porosity configuration.

Given an initial particle distribution, a high porosity exists when the neighbouring particles are not in contact (see Figure 1). The reduction of porosity can be written as a non-linear minimum least-square problem where the function to be minimized is given by the distance between neighbouring particles in the original configuration. This allows the inclusion of boundary constraints to ensure a good reproduction of the boundaries, a feature that constitutes a major advantage in all the cases, where the friction between surfaces is important. Some examples of these conditions are shown by Huang [5] and Zárate *et al.* [4].

In the next section, the basic algorithm where only the internal neighbours are considered is introduced. The next section analyzes the treatment of boundary conditions and constraints, and finally a faster, non-dense initial generation is presented, together with some examples showing the efficiency of the algorithm.

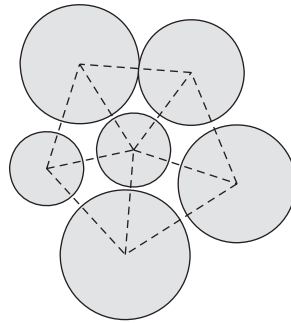


Figure 1. Local neighbourhood of a particle in the interior of the domain.

2.1. Internal contacts

A low-density initial assembly is assumed in order to define the existence of neighbouring particles without contact. The low-density is produced by the void areas where the contacts are not achieved. A modified distance function is defined between all neighbouring particles, where the existence of the contact pair is introduced by a triangulation. In a local neighbourhood for one particle, like the one shown in Figure 1, a distance function between particles i and j can be defined as

$$e_{ij} = \|\mathbf{x}_i - \mathbf{x}_j\|^2 - (r_i + r_j)^2 \quad (1)$$

where \mathbf{x}_i is the coordinate center of the particles i , and r_i its radius. The square of the values is used for the sake of simplicity, because a derivative function is required and the minimum of this modified distance is equivalent to the standard function.

For the central particle i , the sum of the distance to its n_i neighbours is defined as

Register for free at <https://www.scipedia.com> to download the version without the watermark

$$E_i = \sum_{j=1}^{n_i} \|\mathbf{x}_i - \mathbf{x}_j\|^2 - (r_i + r_j)^2 \quad (2)$$

In order to find the minimum of void areas or interstitial spaces, the function E_i needs to be minimized for all the particles in the assembly. For that purpose, a global function is defined using a minimum least-square scheme, where the global function is written as

$$\min F = \sum_{i=1}^m \sum_{j=1}^m \delta_{ij} e_{ij}^2 = \mathbf{E}^T \mathbf{E} \quad (3)$$

where δ_{ij} is a delta function, which takes the value 1 if the contact pair $[i, j]$ exist, and 0 otherwise. These connectivities are achieved by the edges of the triangulation over the initial assembly. The square of e_{ij} is used because the minimum of any contact pair is required, and the use of a linear system may cause some negative values in the radii of the particles. If this solution does not consider contact constraints, then overlapping between particle is allowed. The elimination of the defect will be presented in the next section. The solution of a small example is shown in Figure 2, where the modification of the radii and the center of the particles can be seen.

To solve the minimization problems, an Levenberg–Marquardt scheme is used [18, 19], where the final size and radius of the particles are achieved by the progressive modification of their

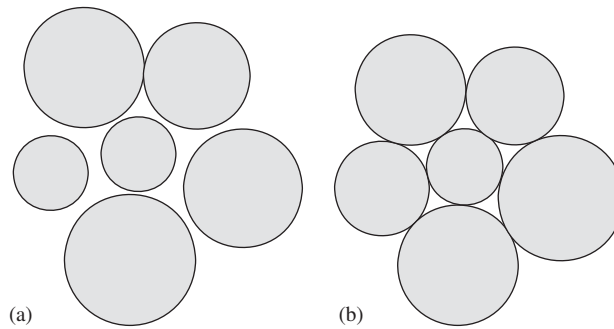


Figure 2. Minimization of the distance in a small assembly of cylindrical particles: (a) initial configuration and (b) final configuration.

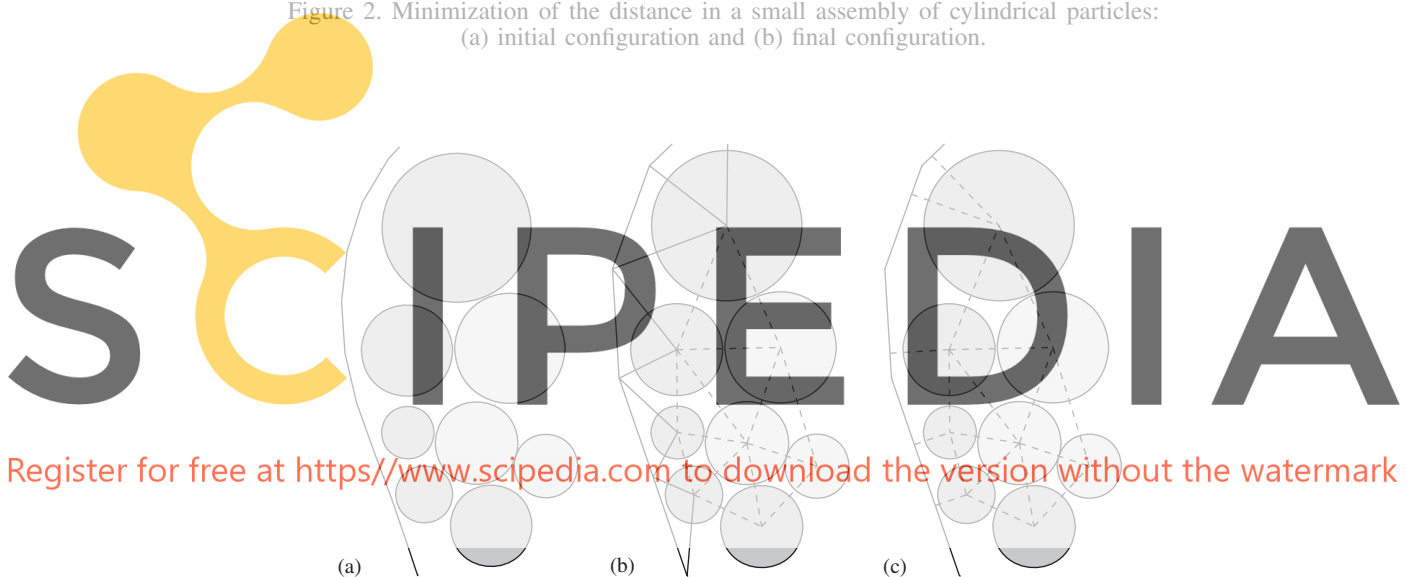


Figure 3. Boundary treatment in the exterior zone of the domain: (a) initial configuration; (b) support mesh; and (c) boundary treatment.

values. The iterative scheme is represented as

$$\mathbf{X}_{k+1} = \mathbf{X}_k + \mathbf{h}_k \quad (4)$$

where \mathbf{X}_k is the vector of degrees of freedom in the iteration k , for a particles package of length n

$$\mathbf{X}_k = [x_1, y_1, r_1, \dots, x_n, y_n, r_n]^T \quad \text{cylindrical particles, 2D} \quad (5)$$

$$\mathbf{X}_k = [x_1, y_1, z_1, r_1, \dots, x_n, y_n, z_n, r_n]^T \quad \text{spherical particles, 3D}$$

The increment vector \mathbf{h}_k is calculated by

$$[\mathbf{J}^T \mathbf{J} + \mu \mathbf{I}] \mathbf{h}_k = -\mathbf{B} \quad (6)$$

where \mathbf{J} is the Jacobian of $\mathbf{E}(\mathbf{J} = \nabla \mathbf{E})$, \mathbf{B} is defined by $\mathbf{B} = \mathbf{J}^T \mathbf{E}$ and μ is a damping parameter.

Equation (6) can be now solved for an initial assembly, where the final compaction degree allows a very low porosity level. The convergence rate of the scheme depends on the initial configuration. A good result is however obtained in few iterations.

For large assemblies of particles, the main computational cost is the solution of Equation (6). For this reason, a faster solver is essential.

2.2. Treatment of boundaries

One of the problems in the generation of the cylindrical or spherical package is the complexity of the geometry. The definition of the boundary is not good for most constructive algorithms. A good definition of the boundary is useful for the simulation of some geomechanics processes where the friction between surfaces is important. An example of this is shown in [4]. The triangulation-based algorithm allows the generation over complex geometries, but not always a good boundary definition is obtained.

A boundary constraint (or boundary condition) is proposed with the same argument as in the previous section. A function of the distance between the contour of the geometry and the external particles is used in order to obtain a homogeneous boundary in the assembly. Figure 3(a) shows an external zone of the domain, where the distance function for particle i and a boundary line k is defined as

$$R_{ik} = \|\mathbf{d}_{ik}\|^2 - r_i^2 \quad (7)$$

where \mathbf{d}_{ik} is the vector joining the center of particle i with the closest boundary point.

We will assume in the following that the algorithm is FEM based. Hence, only the inner nodes of the mesh are particles, whereas the outer nodes define the boundary mesh. With that consideration, it is possible to find a simple way to calculate \mathbf{d}_{ik} , where its value is defined as the projection of the vector defined by the center of particle (x_i) and some of the outer nodes (w_k) along the normal of that boundary element. This is shown in Figures 3(b, c).

The boundary condition (7) is rewritten as

$$R_{ik} = ([\mathbf{w}_k^1 - \mathbf{x}_i] \cdot \mathbf{n}_k)^2 - r_i^2 \quad (8)$$

This allows for each element of the boundary mesh to have a single particle associated with it. Note that in complex zones of the geometry, as acute edges, one particle can have two or more boundary contacts. With the introduction of this new condition, a modified version of Equation (3) is written. Now, the minimization function is defined as

$$\begin{aligned} \min F &= \sum_{j=1}^n \sum_{j=1}^n \delta_{ij} e_{ij}^2 + \sum_{i=1}^n \sum_{k=1}^n \delta'_{ik} R_{ik}^2 \\ &= \mathbf{E}^T \mathbf{E} + \mathbf{R}^T \mathbf{R} \\ &= \mathbf{E}'^T \mathbf{E}' \end{aligned} \quad (9)$$

where δ'_{ik} , just as δ_{ij} , represents the existence of contact between particle i and the boundary element k , and \mathbf{E}' is the new equation system with the boundary functions.

$$\mathbf{E}' = \begin{Bmatrix} \mathbf{E} \\ \mathbf{R} \end{Bmatrix} \quad (10)$$

The resolution of this new minimization problems for a set of particles solved the density problem and yields a good boundary definition for the final configuration of the assembly. Some examples in two and three dimensions are shown in Figures 4 and 5.

One of the advantages of this boundary treatment is that no additional memory is required, because the new term in Equation (6) is included in the diagonal blocks of the global matrix, which are always non-zeros. However, some additional iteration steps are required.

2.3. Particle overlapping

Particle overlapping can arise due to the definition of the distance function adopted. This function is defined so that the total distance between particle pairs is minimum. When the distance between certain pair is large, the minimization process would decrease the value of the global distance function by assigning negative distances to the neighbouring particles, in order to compensate for positive values, as shown in Figure 6(a).

The standard method to avoid this behaviour is to add contact constraints in the minimization problem. However, this method has two drawbacks, the first being its computational cost, and the second that it does not avoid the appearance of overlapping between particles for which contact was not defined in the initial configuration. This phenomenon is depicted in Figure 6(b).

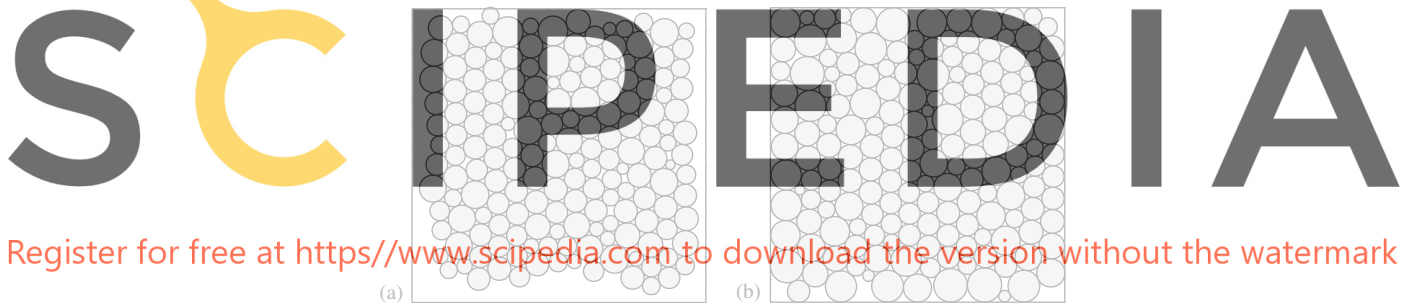


Figure 4. Dense 2D assembly with and without the boundary treatment for a square domain: (a) generation without boundary treatment and (b) generation with boundary treatment.

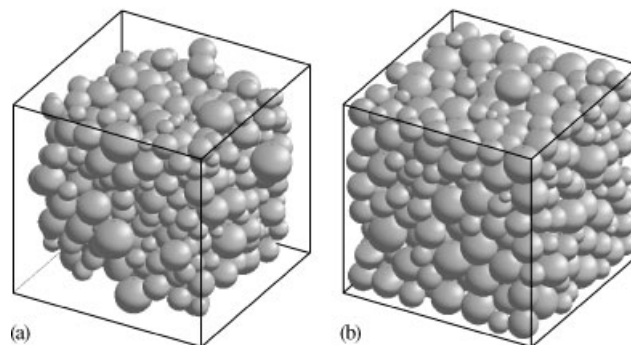


Figure 5. Dense 3D assembly with and without the boundary treatment for cubic domain: (a) generation without boundary treatment and (b) generation with boundary treatment.

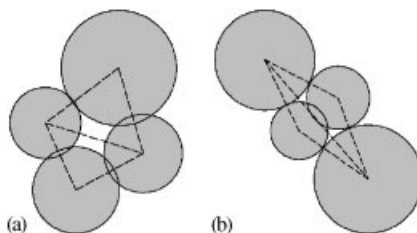


Figure 6. Overlapping over spheres without contact pair definition.

The solution for this problem is to update the contact list and to solve a new distance minimization problem.

The algorithm that updates the contact list can be used to delete those contacts for which the distance is larger than a certain tolerance, which avoids the first type of contact overlapping. In addition, the same algorithm finds the new contact pairs, corresponding to the second type of overlapping described above (Figure 6(b)), which appears in the final configuration after the update process.

Different techniques for updating the contact list can be used. In this work two different approaches have been adopted. The first one is to use of an spatial search algorithm, which requires setting a tolerance for the detecting the contact. The second one consists in the regeneration of the FEM mesh using *weighted delaunay triangulation* [16, 20], which induces a dynamic movement of the mesh.

These modifications require the solution of the distance minimization problem after each update of the connectivities. However, in most cases an acceptable solution is reached after very few steps.

2.4. Initial generation of the media

For the generation of the initial configuration, it is possible to use any algorithm proposed in the literature. However, FEM-based techniques offer better conditions for the algorithm proposed in this work. This is because many well-established algorithms already exist and the generation of complex geometries is achieved easily. A modification of the *Stienen model* is used in our work, where the particles are located in the inner vertex of the mesh and the radii are calculated with a random number over the mean distance between the neighbouring nodes. In addition, the average radius is related to the element size used in the generation of the mesh.

One of the necessary considerations for the initial mesh is the structuration of the elements. A regular element distribution produces a regular number of contacts for the different particles and a homogeneous package of particles is found. In the simulation of geomechanical processes that deal with the particle cohesion, a structured lattice of particles can be problematic because small forces can lead to material fracture. In order to solve this problem, an initial preprocessing is performed over the mesh, where random local displacements over the node position are used to generate a random configuration. After this perturbation, a new triangulation is used for defining the contact pairs. An example of the initial mesh and its modification is shown in Figures 7 and 8.

In order to define the size of the particles, the average distance between nodes is calculated and a random number generator modifies these values with a user-defined range. Overlapping is allowed, because the optimization of the distance between particles eliminates these defects.

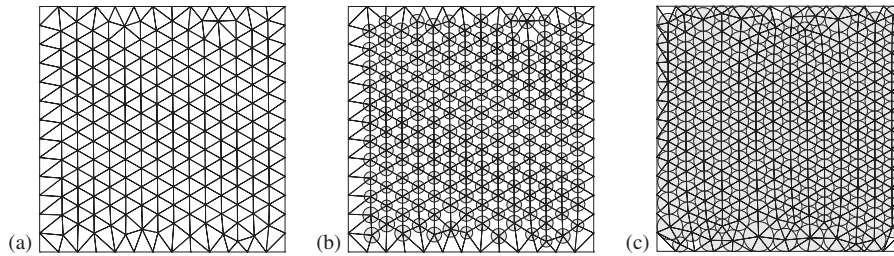


Figure 7. Generation with structured mesh for the initial configuration: (a) structured mesh; (b) initial configuration; and (c) final configuration.

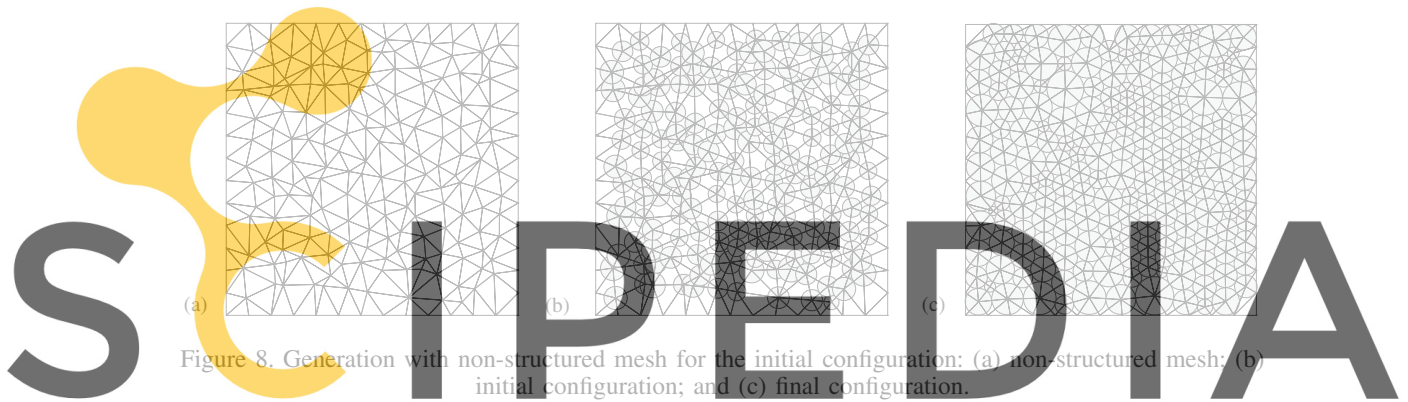


Figure 8. Generation with non-structured mesh for the initial configuration: (a) non-structured mesh; (b) initial configuration; and (c) final configuration.

Register for free at <https://www.scipedia.com> to download the version without the watermark

5. CHARACTERIZATION OF RESULTS AND EXAMPLES

In order to compare different packing algorithms, it is necessary to use some parameters that indicate the quality of the generated media. In the literature, several parameters can be found in order to analyze the quality of the results.

In dense particle assemblies, parameters like *average radius*, *void ratio* or *coordination number* are used. Other useful parameters exist, but none of them was used for the following comparisons. An introduction to some of these parameters can be found in [21, 22].

The *average radius* is calculated as

$$r_{\text{avr}} = \sqrt{\frac{\sum_i r_i^2}{N_p}}$$

The *void ratio* indicates the relationship between the volume achieved by the generation process V_v and the real volume of the geometry V_s .

$$e = 1 - \frac{V_v}{V_s}$$

This allows to determine the relative density of the packaging.

The *coordination number* expresses the contact between particles in order to determine the existence of cohesion in the particle assembly.

$$c = \frac{2N_c}{N_p}$$

with N_c being the total number of contacts between the N_p particles of the generated packaging.

A set of results is obtained by considering different sizes of particles in a square domain in 2D and in a cubic domain in 3D (similar to the examples shown in Figures 4 and 5). A 3 GHz Pentium 4 is used to compute the examples.

Table I. Comparison of 2D cylindrical particles generation.

Algorithm	N_p	r_{avr}	e (%)	c	Time
PFC2D	–	0.259	13.1	4.34	64 h
Bagi [23]	56 213	0.221	14.2	3.98	388 s
Present algorithm	56 084	0.223	9.3	5.97	118 s

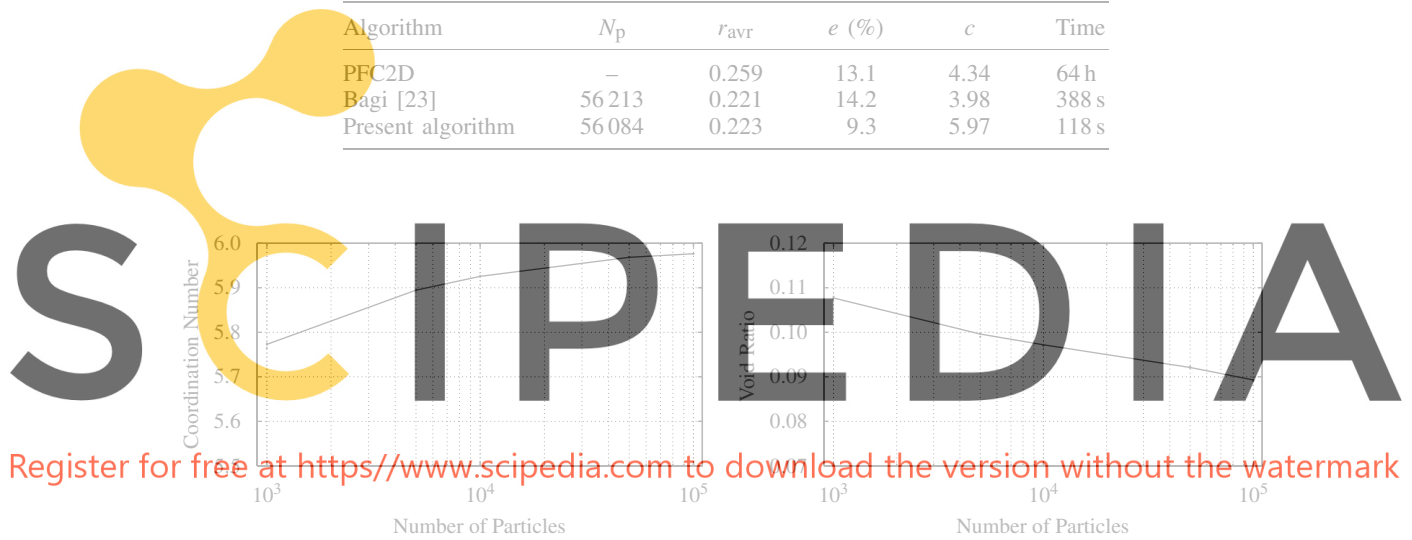


Figure 9. Coordination number and void ratio for different numbers of particles.

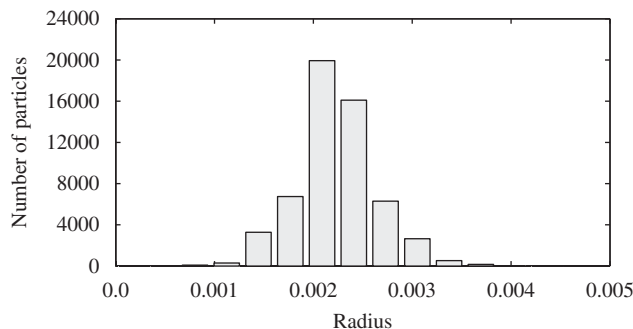


Figure 10. Radii distribution for cylindrical particles. The values correspond to the generation of 56 213 particles presented in Table I.

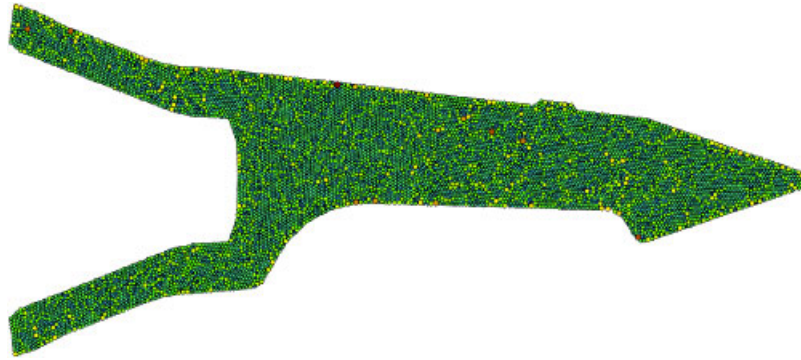


Figure 11. Tooth of the excavation machine discretized with 10 000 cylindrical particles.

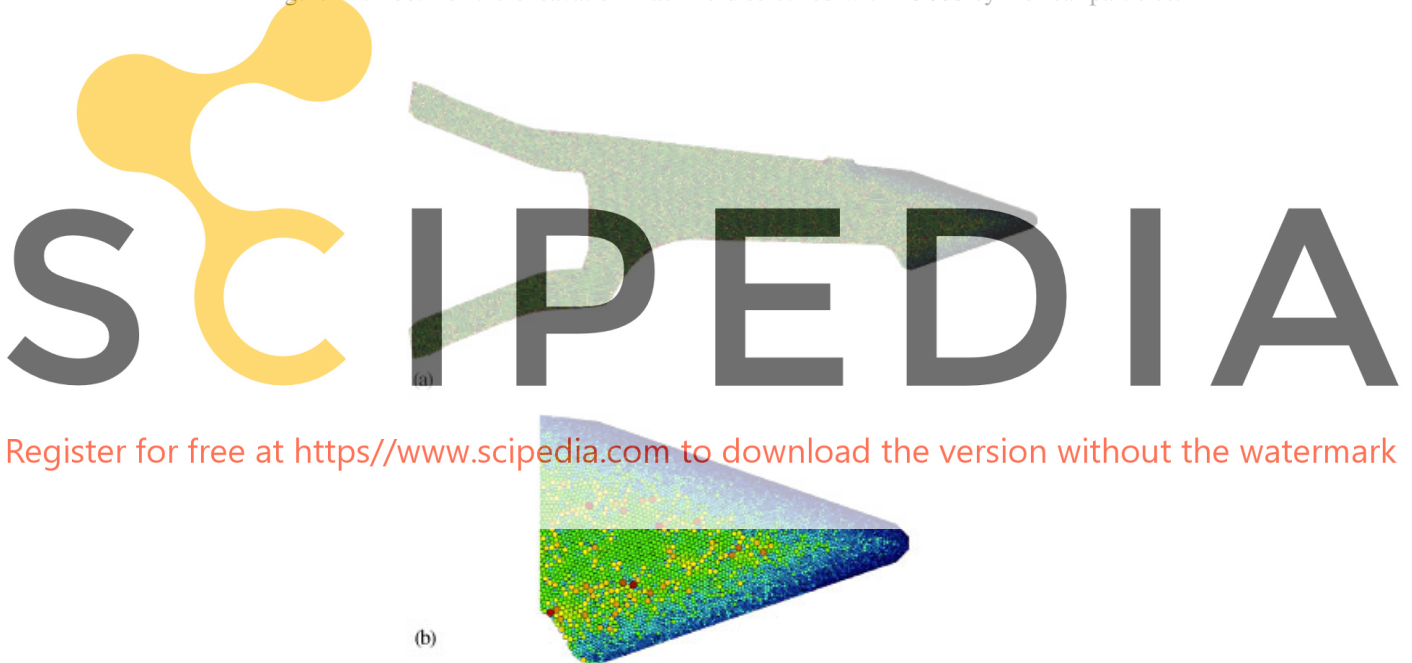


Figure 12. Tooth of the excavation machine discretized with cylindrical particles and refinement in the external surface: (a) discretization with 23 500 cylindrical particles and (b) detail of refined zone.

The above non-dimensional parameters are used in order to determine the quality of the generation. Comparisons with the results obtained by Bagi [23] are also made. The values reported for the PFC2D code can be found in the same paper. Table I shows that the proposed algorithm achieves a better result, as the porosity is significantly lower than for the other algorithms.

For a structured mesh, the mean number of neighbours is 6. The initial random displacement in the mesh modifies that number, but a similar number of neighbours are achieved. This produces a high coordination number, while the minimization of the distance between neighbour particles decreases the porosity values.

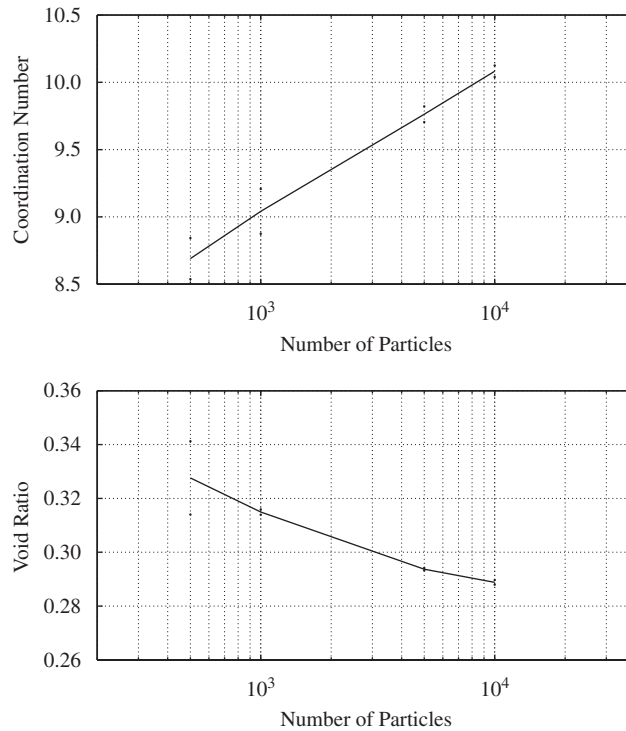


Figure 13. Coordination number and void ratio for different number of spherical particles.

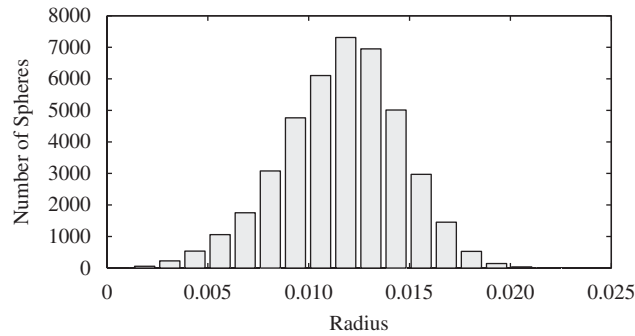


Figure 14. Radius distribution for 50 000 spheres.

The values of the void ratio and the coordination number for different number of 2D particles are shown in Figure 9. Note the fast decrease of the porosity as the number of particles increases. The distribution of radii, for the case presented in Table I, is shown in Figure 10. A Gaussian distribution can be observed in most of the cases.

Figure 11 shows an example of the discretization of a tooth of an excavation machine with 10 000 particles.

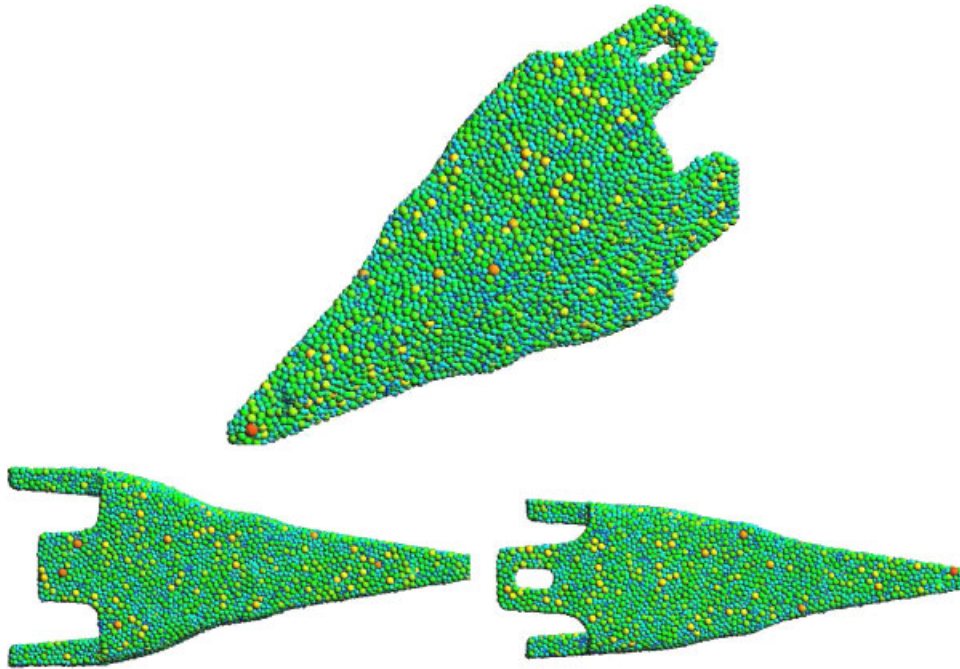


Figure 15. Tooth of excavation machine. 3D discretization.

A local refinement in the zone where surface wear is expected to occur is presented in Figure 12. The use of FEMs with refinement and the local parameters for the generation allows a good result for this type of problems.

For 3D generation, the coordination number and porosity for different numbers of particles are shown in Figure 13. The decrease of the porosity for a high number of particles can be observed. A good number of neighbours is achieved in a similar way as for the 2D case. The radii distribution for an example with 50 000 spheres are shown in Figure 14.

Finally, an application example is shown in Figure 15. Similar to the 2D example, a tooth of an excavation machine is discretized with 25 000 spherical particles. A good result of the generation process can be observed. The final porosity found in this case is 30.77%.

4. CONCLUSION

A new dense sphere particle packing algorithm has been presented. The search of a low porosity configuration for an initial sphere assembly is performed using a minimization scheme for the distance between adjacent particles. The contact pairs definition is carried out using a triangulation technique. A boundary constraint is included in order to obtain a good surface definition. This allows the fine discretization of complex geometries. For the generation of the initial configuration, a faster FEM-based scheme is used. The comparison with other algorithms shows good result for the porosity and coordination number obtained with a considerable speed.

The particle packing technique presented is a good candidate for problems, which require high-density packing.

ACKNOWLEDGEMENTS

The authors thank Jerzy Rojek and Facundo del Pin for their advice during this work.

REFERENCES

1. Cundall PA. Formulation of a three dimensional distinct element model—part i. A scheme to detect and represent contacts in a system of many polyhedral blocks. *International Journal of Rock Mechanics, Mining Sciences and Geomechanics Abstracts* 1988; **25**(3):107–116.
2. Cundall PA, Strack ODL. A discrete numerical method for granular assemblies. *Geotechnique* 1979; **29**:47–65.
3. Zarate F, Rojek J, Oñate E, Miquel J. Modelling of rock, soil and granular materials using spherical elements. In *ECCM-2001, CD-ROM Proceedings of the Second European Conference on Computational Mechanics: Solids, Structures and Coupled Problems in Engineering*, Waszczyszyn Z, Pamin J (eds). Cracow, 2001.
4. Zarate F, Rojek J, Oñate E, Miquel J. Thermomechanical discrete element formulation for wear analysis of rock cutting tools. *Technical Report*, CIMNE, Barcelona, 2004.
5. Huang H. Discrete element modeling of tool–rock interaction. *Technical Report*, University of Minnesota, 1999.
6. Oñate E, Rojek J. Combination of discrete element and finite element methods for dynamic analysis of geomechanics problems. *Computer Methods in Applied Mechanics and Engineering* 2004; **193**:3087–3128.
7. Labra C, Rojek C, Oñate E, Zarate F. Advances in discrete element modelling of underground excavations. *Acta Geotechnica* 2008; DOI: 10.1007/s11440-008-0071-2.
8. Itasca. *PFC2D 2.00 Particule Flow Code in Two Dimensions*, Minneapolis, MN, 1998.
9. Lin X, Ng T-T. A three-dimensional discrete element model using arrays of ellipsoids. *Geotechnique* 1997; **47**(2):319–329.
10. Evans JW. Random and cooperative sequential adsorption. *Reviews of Modern Physics* 1993; **65**:1281–1304.
11. Häggström O, Meester R. Nearest neighbour and hard sphere models in continuum percolation. *Random Structures and Algorithms* 1996; **9**:295–315.
12. Stoyan D. Random set: models and statistics. *International Statistical Review* 1998; **66**:1–27.
13. Cui L, O’Sullivan C. Analysis of a triangulation based approach for specimen generation for discrete element simulation. *Granular Matter* 2003; **5**:135–145.
14. Feng YT, Han K, Owen DR. Filling domain with disk: an advancing front approach. *International Journal for Numerical Methods in Engineering* 2003; **56**(5):699–731.
15. Lohner R, Oñate E. A general advancing front technique for filling space with arbitrary objects. *International Journal for Numerical Methods in Engineering* 2004; **61**:1977–1991.
16. Ferrez JA. Dynamic triangulation for efficient 3D simulation of granular materials. *Ph.D. Thesis*, Ecole Polytechnique Federale de Luusanne, Lausanne, 2001.
17. Han K, Feng YT, Owen DR. Sphere packing with a geometric based compression algorithm. *Powder Technology* 2005; **155**:33–41.
18. Levenberg K. A method for the solution of certain problems in least squares. *Quarterly of Applied Mathematics* 1944; **2**:164–168.
19. Marquardt D. An algorithm for least square estimation on nonlinear parameters. *SIAM Journal on Applied Mathematics* 1963; **11**:431–441.
20. Ferrez J-A, Liebling ThM. Robust 3d dynamic triangulations for collision detection in dem simulations of granular materials. *EPFL Supercomputing Review* 2002; **13**:41–48.
21. Cambou B. *Micromechanical Approach in Granular Mechanics*. Behaviour of Granular Materials, vol. 385. Springer: Berlin, New York, 1998.
22. Luding S. Micro–macro transition for an-isotropic, frictional granular packings. *International Journal of Solids and Structures* 2004; **41**(21):5821–5836.
23. Bagi K. An algorithm to generate random dense arrangements for discrete element simulations of granular assemblies. *Granular Matter* 2005; **7**:31–43.